Journal of Cultural Heritage 67 (2024) 9–22

Contents lists available at ScienceDirect

Journal of Cultural Heritage

journal homepage: www.elsevier.com/locate/culher

VSI: TECHNART 2023 selected papers

Historical silks: a novel method to evaluate their condition with ATR-FTIR spectroscopy and Principal Component Analysis

Ludovico Geminiani[a,c,*], Francesco Paolo Campione[b,c,d], Cristina Corti[b,c], Barbara Giussani[a], Giulia Gorla[e], Moira Luraschi[c,d], Sandro Recchia[a], Laura Rampazzi[b,c,f]

[a] Dipartimento di Scienza e Alta Tecnologia, Università degli Studi dell'Insubria, Via Valleggio 11, 22100 Como, Italy
[b] Dipartimento di Scienze Umane e dell'Innovazione per il Territorio, Università degli Studi dell'Insubria, Via Sant'Abbondio 12, 22100 Como, Italy
[c] Centro Speciale di Scienze e Simbolica dei Beni Culturali, Università degli Studi dell'Insubria, Via Sant'Abbondio 12, 22100 Como, Italy
[d] Museo delle Culture, Villa Malpensata, Riva Antonio Caccia 5, 6900 Lugano, Switzerland
[e] Research and Innovation in Analytical Chemistry group (IBeA), Departamento de Quìmica Analìtica, University of Basque Country, Barrio Sarriena, s/n, 48940 Leioia - Bizkaia, Spain
[f] Istituto per le Scienze del Patrimonio Culturale, Consiglio Nazionale delle Ricerche (ISPC-CNR), Via Cozzi 53, 20125 Milano, Italy

ARTICLE INFO

Article history:
Received 28 October 2023
Accepted 31 January 2024

Keywords:
Condition assessment
Silk
Silk degradation
ATR-FTIR spectroscopy
PCA
Historical textiles

ABSTRACT

Understanding the conservation condition of historical silk yarn allows to define appropriate storage, care and display of historical silk collections. This paper discusses the characterisation of silk fabrics from a collection of traditional Japanese samurai armours which date back from the 16th to the 20th century (Morigi Collection, Museo delle Culture, Lugano, Switzerland). An analytical protocol to assess silk fabrics conditions was defined, based on microinvasive ATR-FTIR spectroscopy. In particular, the amide I and II region was studied in order to extrapolate the conformational information about silk proteins. According to literature, this kind of information can be related to different degradation stages. A linear correlation was found between the amide I and the amide II shifts, allowing to assess the silk fibre condition. Along with this bivariate approach based on intensity ratios, a multivariate approach based on Principal Component Analysis was also applied to ATR-FTIR spectra. This allowed to group together silks with the same state of preservation. The findings of this research offer a valuable method to researchers and conservators to identify the most damaged textiles; the differentiation between original and restoration materials was also possible in some cases.

1. Introduction

The preservation of objects in museums and other cultural heritage institutions is crucial to ensure their legacy to future generations. To appropriately care for a wide range of cultural heritage materials, the assessment about their nature and their condition should be planned, preferably by means of micro- and non-invasive analytical techniques [1]. Rigorous scientific research can not only extend the life of historical artifacts but also provide an opportunity to delve deeper into the understanding of a collection, thereby enriching its historical significance. This is particularly true for textiles [1], which embody a significant part of our shared heritage. Textiles can encapsulate the evolution of techniques, the mastery of artisans, and the influences of trade and cultural exchanges. Nonetheless, in many cases textile artifacts are in a rather deteriorated state. Many of them were initially designed as practical, utilitarian objects, so they endured the wear and tear of daily use. The materials used in crafting these items, primarily vegetable or animal fibres, tend to be relatively fragile and susceptible to deterioration caused by a variety of chemical and physical processes. Deterioration factors are further exacerbated by any adverse occurrence, including mechanical stress, encountered throughout the objects' lives. Consequently, very few items make their way into collections in a pristine condition.

Silk is reported as one of the most vulnerable materials within natural and synthetic fibres, particularly when exposed to light [2]. The origins of silk date back to ancient China; it played a pivotal

* Corresponding author.
E-mail addresses: lgeminiani@uninsubria.it (L. Geminiani), cristina.corti@uninsubria.it (C. Corti), laura.rampazzi@uninsubria.it (L. Rampazzi).

https://doi.org/10.1016/j.culher.2024.01.015

role in connecting civilizations through the Silk Road [3] and its trade fostered cross-cultural exchanges and influenced the development of art and fashion. The intricate processes involved in the production of silk reflect the scientific and technical achievements of past civilizations. Silk has not only been cherished for its inherent beauty but also for the rich hues obtained through the dyeing process. Before being dyed, silk generally undergoes the degumming process, which is used to remove the gum covering the yarn and make the silk smooth and lustrous. After this process, the silk is named soft or degummed. If gum is not completely removed, the silk is named hard. Hard silk is more difficult to dye, and its colours are not so vivid, but it shows a higher tensile strength [4]. Hard silk was used in the early stages of sericulture, but also when the fibre strength was to be prioritised over its aesthetics. In Japan, silk was extensively used in the traditional samurai armour, especially in order to make the *odoshige* (lacing amongst metal plates) and for linings brocades [5]. The life of an armour was remarkably dependant on the periodic renovation of its lacing: the deterioration of silk, which carried the weight of the metal parts of the armour, was inevitable [6]. In modern days, conservators can design supports to carry the weight of the metallic components of the armour without putting the degraded textiles under stress. Similar strategies could be applied to mount textiles for display, especially when a vertical display is required, which is the most dangerous for the fabrics [7]. It is therefore important to appropriately assess the condition of such textiles, to improve conservation effectiveness. Besides, the information could be also useful to differentiate modern restoration from the original manufacturing.

Silk is commonly characterised by distinctive features, such as smoothness and lustre. By a visual inspection, viscose can be easily mistaken for silk, as it was firstly developed as a cheap cellulose-based substitute for silk [2]. Also mercerized cotton and polyester were used to mimic silk, as demonstrated by the ongoing analyses performed on the collection object of this investigation. Fourier Transform Infrared (FTIR) spectroscopy is a well-known tool for the identification of fibres [2,8]: for example, viscose is easily distinguished from silk [9], as viscose is derived from cellulose and silk is protein-based [10]. Since the first studies in the 1950s by Asai [11] and Miyazawa [12], traditional transmission FTIR spectroscopy has proved to be a sensitive technique for silk fibroin. The main FTIR absorption bands of silk are due to the absorptions by amide A, B, I, II, and III, which are characteristic for the protein backbone [13]; alongside these absorptions which are common to all proteins with little variations, other signals arise from the amino-acids side chains, such as ν(CC) and δ(CH) in tyrosine, ν(C = O) in aspartic acid, and ν(CO) in serine [13–15]. Organic polymeric materials such as proteins are affected by a variety of deterioration agents. Silk in particular is heavily affected by light [16]. On top of that, silk processing very often involved treatment with mordants which could also cause or catalyse deterioration [17]. The initial phase of ageing of silk is characterized by the formation of new compounds and by the stabilisation of the fibre. Finally, evident degradation can be observed, through yellowing and embrittlement [2,18]. More information is given in the Theory section. Chemical and physical agents can induce modification in proteins, influencing their secondary structure – the geometry a polypeptide chain takes according to its primary structure [13]. These changes are visible in the infrared spectrum of proteins, as the amides I and III bands of polypeptides and proteins (but also amide II) [19] are sensitive to changes in the secondary structure. IR spectroscopy can distinguish α-helix, β-sheet, β-turns, and disordered structures [13]. As the relative percentages of each secondary structure vary with degumming, ageing and degradation [20], it appears of great importance to find estimators to compare slightly different spectra. FTIR peak areas, which can be obtained by applying a peak fitting algorithm, or peak intensities are both employed. Generally, Attenuated Total Reflection (ATR) FTIR data are evaluated. The quantification of conformation change is possible through the evaluation of the areas [13,21]. Alternatively, the peaks intensities can be calculated as ratios and correlated to the degree of crystallinity, oxidation index and other structural properties, giving a qualitative tool to compare spectra [22–27]. Recently, the chemometric approach was proposed to evaluate spectral data from historical silk samples. Some research works applied Principal Component Analysis (PCA) in order to highlight trends and to visualize the variability of data [24,25].

2. Research aim

Infrared spectroscopy and an easy-to-use chemometric technique were chosen in this research to gain an insight into the degradation of historical samples of silk. Our work was designed as a part of a challenging work of characterisation of a large selection of historical materials of a collection of Japanese traditional armours belonging to Morigi Collection (Museo delle Culture, Lugano, Switzerland). During the study of the textiles belonging to this collection [9,28,29], some correlations between the state of preservation of silk samples and their measurable spectroscopic signatures were highlighted. These markers were interpreted and supported by theoretical research on the ageing of silk. Experimental data were investigated through a bivariate approach based on intensity ratios and as well as through a multivariate approach based on Principal Component Analysis applied to ATR-FTIR spectra. Both approaches aimed to define a novel and simple method to assess the deterioration state of the silk fibres, through a micro-invasive methodology. Yielding information on the degradation condition could be very useful to determine suitable approaches to conservation treatments, display and storage strategies for silk textiles. This study can also provide valuable information to support authenticity and dating studies.

3. Materials and methods

3.1. Reference materials

Modern reference samples of unaged hard (non-degummed) and soft (degummed) *Bombyx mori* silk were obtained from 'Centro Tessile Serico Sostenibile' (Como, Italy).

3.2. The Morigi Collection of traditional Japanese armours

The silk samples, object of this research, belong to the Morigi Collection, which is composed of nine Japanese full armours and a set made by a helmet (*kabuto*) and a masque (*menpō*). More information about the collection is available in Appendix A. 28 samples, generally only a few millimetres long, were taken paying attention to avoid creating any visible damage, from previously damaged or hidden areas. It was not possible to sample from some of the armours. The samples were collected using scissors and tweezers and stored in plastic (LDPE) containers until analysis in the laboratory. The analysed armours and the corresponding samples are listed in Table 1, while the samples are shown in Fig. 1.

3.3. Attenuated Total Feflectance Fourier Transform Infrared spectroscopy

ATR-FTIR spectra were acquired with a Thermo Scientific Nicolet iS10 instrument, in the range between 4000 and 600 cm^{-1}, with 4 cm^{-1} resolution and 32 scans acquisition. The background was periodically acquired and subtracted, in order to remove the atmospheric air contribution. The choice of resolution and number of scans to be used was made on the basis of preliminary tests

Table 1
List of the samples taken from the armours of the Morigi collection.

Armour	Samples	Armour type	Presumed dating
2017.Mor.1	1_6, 1_8 g, 1_8b	*kinsei gusoku*	late 16th c.
2017.Mor.3	3_4	*kinsei gusoku*	17th c. (*kabuto*: late 16th c.)
2017.Mor.4	4_1, 4_6, 4_7c, 4_7d, 4_7e, 4_7f, 4_7 g, 4_8c, 4_8 s, 4_9, 4_10 g, 4_10b	*mukashi gusoku*	18th c. (*suneate*: late 16th c.)
2017.Mor.6	6_2	*kinsei gusoku*	early 20th c.
2017.Mor.7	7_1f, 7_1b, 7_1 g	*kinsei gusoku*	late 16th c.
2017.Mor.8	8_4, 8_8	*kinsei gusoku*	17th c.
2017.Mor.9	9_2, 9_4, 9_5b, 9_5ve, 9_5vi, 9_5r	*mukashi gusoku*	late 19th c.

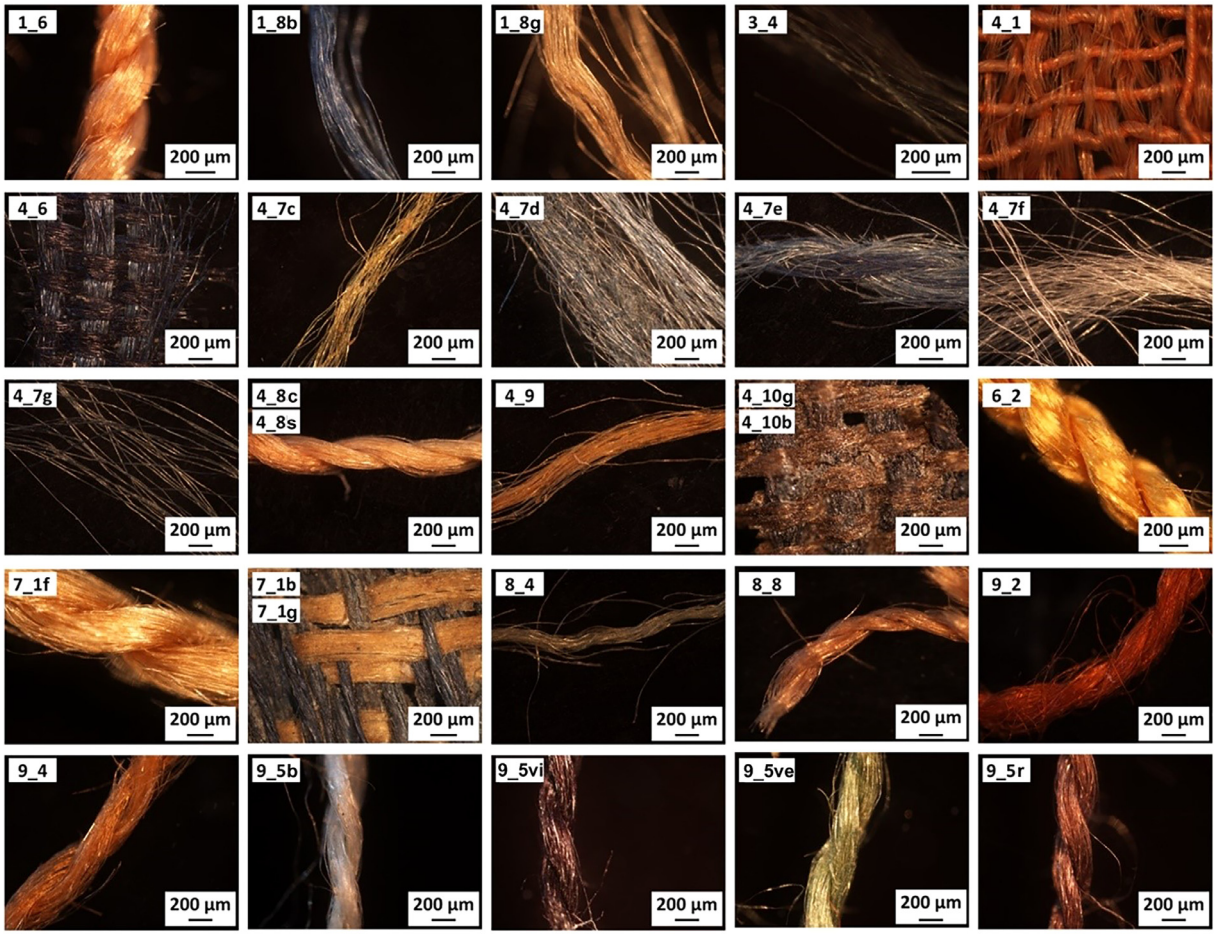

Fig. 1. Optical microscopy images of the samples taken from the armours. Sample labels are shown in the upper left corner of the images.

carried out under different measurement conditions. The chosen settings appear to be those that allow significant spectra to be obtained while at the same time optimising analysis time.

3.4. Data treatment and elaboration

Spectra were interpreted by comparison with a custom-made reference database and with the available literature. Microsoft Excel 2023 was used to do bivariate calculations. Origin Pro 2018 was used to draw the graphs. Spectragryph optical spectroscopy software, Version 1.2.15, was used to visualize and process the ATR-FTIR spectra, and also to extrapolate the intensity values of the spectra [30]. Before comparing the spectra, they underwent the following process: i) spectrum truncation to the region 1800–1400 cm^{-1}, ii) baseline correction by removing a linear function connecting the two extremes of the truncated spectra, iii) spectrum normalization by area, i.e. the integral for the interval 1800–1400 cm^{-1} was set to a common value.

This standardized approach was suggested by previous works using peak fitting analysis [19,21] and was consistently applied to all spectra without any modifications. The spectral region which was subjected to linearization was chosen after extensive testing, due to the risk to create spectrum distortions with baseline correction. Similarly, the possibility of pressure-induced structural changes in silk fibroin due to the ATR-FTIR instrument was taken into account and tested, as reported by some authors [21]. The consistent use of the same instrument under identical measuring conditions for all samples assures us that any potential alterations, although remote, are constant across all samples. The application of the normalization algorithm was used to compensate for the differences in the intensities of the spectra and make them comparable. This was made on the hypothesis that the infrared absorption coefficient of silk during ATR-FTIR analysis was equal for all the samples. The thickness of the analysed silk textiles is not constant, and the literature reports the deep influence of the thickness of the silk fibre on the intensity of the ATR-FTIR spectrum [31].

3.5. Principal component analysis

Principal Component Analysis (PCA) was applied to the ATR-FTIR datasets. Standard Normal Variate (SNV) was applied to data as a preprocessing method to eliminate the nonspecific signal due to light scattering with the textile surface. All data were centred before further analysis, as common before any chemometric calculations. The software used for chemometric calculations was R version 3.6.3 (RStudio version 1.4.1106). PCA scores were evaluated by comparison with the results of spectra evaluation. In scores plot, which is the map of samples in the space described by the PCs, samples lying close together have similar characteristics, while spatially distant samples are samples with different features. The loadings provide indications of the factors that differentiate them, indicating which variables are most effective in distinguishing one sample from another. The variables with high loadings (in absolute value) are those that mainly differentiate the samples.

3.6. Optical and scanning electron microscopy

The thread samples were observed with an optical microscope Nikon Eclipse LV150, equipped with a Nikon DS-FI1 digital image acquisition system. Images were acquired and elaborated using the NIS-elements F software. The samples were observed without any pre-treatment with a FEI/Philips XL30 ESEM (low vacuum mode - 1 torr, 20 kV). Images were taken in backscattered electron (BSE) mode.

4. Theory

Fibroin and sericin are the main proteins that form *Bombyx mori* silk fibres [32]. Sericin is generally eliminated in order to obtain a smooth and shiny yarn, which is named soft or degummed silk. Fibroin [2] is composed mainly of glycine, alanine and serine, in a proportion of 3:2:1. These small amino acids provide fibroin with high packing-efficiency, so that the majority of fibroin is crystalline. The presence of minor amino acids such as arginine, threonine, tryptophan, phenylalanine and tyrosine, which cannot be accommodated in the crystalline domains, causes the appearance of an amorphous phase amongst crystallites. Aromatic amino acids, such as tyrosine, are particularly sensitive to UV light, so tyrosine gradually disappears during ageing [23] and generates radicals affecting the backbone. This makes silk the most UV-sensitive natural fibre [2]. The degradation pathway of silk is known from a chemical point of view [2]. Different degradation agents (UV, heat, moisture, alkalis, acids, biological agents, mechanical stress) can affect the peptide backbone or amino-acid residues. Many studies about fibroin ageing showed that the material undergoes various conformational transitions before final degradation [16,33,34]. When silk fibroin is solubilized in water and then let to crystallize again on a surface, it can take three forms depending on the concentration and the casting. The three forms are random coil, α-helix or β-sheet. It was demonstrated that the random coil to β-sheet transition is promoted by a lot of conditions, i.e. heating [35,36], UV exposure [24,37], treatment with hydrophilic solvents such as ethanol [35,38,39] and heated water [40]. Similarly, a slight increase of β-sheets is reported in the initial stages of degradation induced by UV light, which historical silks are most likely to experience. This stage is also characterized by the decrease of random coil and α-helix conformation and the increase of β-turns [24,34,41]. It is generally believed that in these early stages the UV radiation affects mainly the amorphous phase. The percentage of the crystalline phase increases accordingly [16,26,33]. As a matter, the crystallites adopt an antiparallel β-sheet conformation, while the structural organization in the amorphous phase is not well understood yet, probably showing a β-turns or a disordered structure. As degradation progresses, the action of UV radiation decreases the size of β-sheet crystallites, and finally transforms them to random coil. At this point the mechanical properties of silk textile are lost [26,34,42,43].

5. Results and discussion

5.1. Overview

ATR-FTIR spectra of analysed samples allowed an easy identification of the samples as proteinaceous fibre, according to main absorption assigned to amide vibrations [13]. To distinguish silk from other natural and synthetic polypeptides, the spectra were evaluated in comparison with a degummed silk reference. Band assignment for fibroin was discussed in a previous work on silk [29]. The spectra of the majority of the samples strictly resembled the one of the silk reference, even if some major differences appeared in few samples. Firstly the presence of sericin was evaluated, as one of the main differences during the processing of silk is the degree of degumming. Our previous research into silk degumming assessment [29] identified some spectral features which are distinctive to hard (non-degummed) silk. These features were not assessed, so the presence of other materials was investigated. In summary, four samples showed the characteristic spectral features from a polysaccharidic material, other four samples indicated the presence of gypsum, and finally sample 9_2 was found to contain rosin and talc. The presence of gypsum did not prevent further processing of the spectrum, while other samples could not be further investigated, as the FTIR absorption bands of other materials appeared in the spectral regions object of this investigation. When researching on historical textiles, attention should be paid to the presence of such materials, as they could hinder further processing of the spectra. The FTIR results are discussed extensively in Appendix B.

5.2. Classification according to the amide bands shift (bivariate method)

After the assignment of the main peaks and the identification of the major differences amongst the spectra, the minor variations were also compared. In particular, in the 1800–1400 cm^{-1} region, some of the samples, such as samples 4_1 and 6_2 (Fig. 2) show clear shifts in the maxima from 1617 to 1626 cm^{-1} (amide I peak) and changes in intensity at 1516 and 1503 cm^{-1} (amide II peak). It is interesting that sample 6_2 is similar to both hard (non-degummed) and soft (degummed) silk references, while sample 4_1 differs from the others in the peaks position and intensities. The position and the intensities of the peaks of hard silk spectrum (HS) are similar to soft silk spectrum (SS), so the shift could not be related to the content of sericin, as it was explained in a previous work [29]. Even if changes are minimal, the shift in amide I peak at around 1620 cm^{-1} can be clearly recognized and is consistent with literature, suggesting that the shift is caused by a conformational change in the secondary structure of silk proteins [44].

In order to explain such a difference, changes occurring to the secondary structure during ageing should be considered. The amide group in proteins, including fibroin and sericin, presents characteristic vibrational modes called Amide modes. Amide I band in 1700–1590 cm^{-1} region can be attributed to C=O stretching vibrations, amide II in 1590–1460 cm^{-1} region to N–H bending and C–N bending vibrations, and amide III in 1190–1280 cm^{-1} region to N–H bending and C–N stretching vibrations. These broad bands are constituted by the superimposition of many signals arising from the conformational structure of fibroin, which can change due to the exposure to heat, light and chemicals. Table 2 presents the main assignments for silk fibroin in the region of amide I, II, and

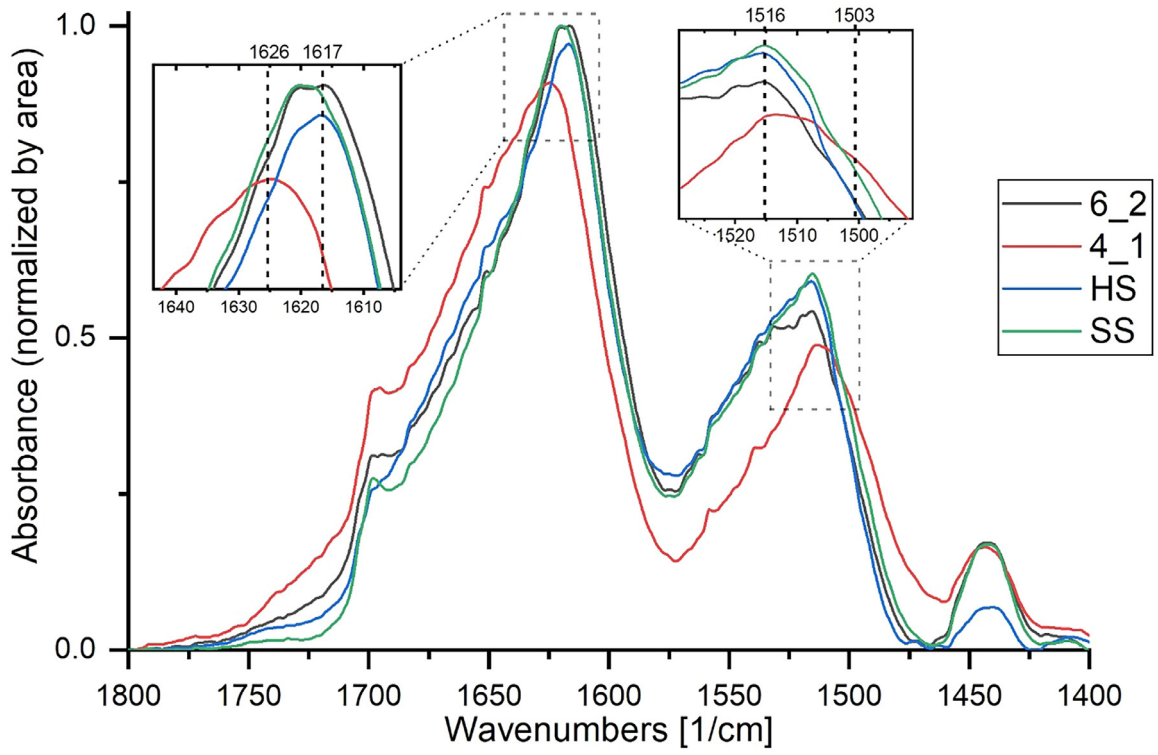

Fig. 2. ATR-FTIR spectra of samples 6_2 and 4_1 versus spectra of unaged hard silk (HS) and soft silk (SS) reference materials. The vertical lines highlight the shifts of amide I and II peaks.

Table 2
Band assignment for fibroin and sericin in the spectral range of amide I, II and III.

Wavenumbers (cm^{-1})	Main assignment	Alternative assignment
1720–30	oxidation products [22,45]	
1698	intermolecular β-sheet [12,38,44,46]	β-turn [47]
1680–1668	β-turn [44,46]	
1656–1662	α-helix [35,44,46,48]	
1639–1655	random coil [38,44,46]	
1628–1637†	intramolecular β-sheet [13,35,44,46–48]	
1627–1622†	intermolecular β-sheet [44,45,46,49]	
1621–1616	aggregated β-strand/intermolecular β-sheet (weak) [44]	
1615–1605	ν(CC) + δ(CH) of tyrosine [13,14,44,50]	
1602–1595	ν(CC) of tyrosine [13,44,51]	
1555	Tyrosine [14]	β-sheet [51]
1545	α-helix, random coil [12,35,48,52]	
1530‡	β-sheet [12,35,48,52]	α-helix, random coil [51]
1515	ν(CC) + δ(CH) of tyrosine [13,14,50–52]	
1508	β-sheet [51,53]	
1260	β-sheet [47,48]	α-helix [35]
1230	random coil, α-helix [47,48]	β-sheet [35]

† : some authors [54,55] report that a shift is observed from around 1640 cm^{-1} (transmission mode) to around 1620 cm^{-1} (ATR mode).
‡ : until the 1990s, some authors recognized two peaks: 1525–1530 cm^{-1}, assigned to β-sheet, and 1535–1540 cm^{-1} assigned to random coils [35,48]. This could be related to the use of traditional transmission spectrophotometer (not ATR) [56]. Calculated frequencies of amide II for a polypeptide in various conformations are 1535 and 1540 cm^{-1} for random coil or α-helix and 1530 cm^{-1} for β-sheet.

III. The literature on the topic is wide, so sometimes attribution is not unanimous. The current work relied on the main assignment, but alternative assignments are also reported. Fibroin and sericin mostly show the same bands [29].

Each conformation gives rise to different signals within the band. It happens because each conformation shows different length of hydrogen bonding and the strength of C=O and N–H bonds, from which the signal is generated, is strongly influenced by hydrogen bonding [13,44,49]. In particular, the frequency of these vibrations is as lower in wavelength as stronger are the hydrogen bonds involved in the carbonyl groups. As for the amide I peak, the shift in C=O absorption maximum is explained as follows. If fibroin had shown a totally crystalline behaviour, with an intramolecular β-sheet conformation (N–H···O=C hydrogen bonds within folded strand of the same chain), the main signal would have appeared at 1630–40 cm^{-1}. However, such structure is contained only in crystalline domains, which are surrounded by extended chain and random coil structures. Thus, the main absorption is expected to appear at around 1620 cm^{-1}, as seen in the spectra. The peak maximum at 1620 cm^{-1} is an indicator of the high content of intermolecular β-sheets, which are planar, extended chains able to align extremely well with neighbouring chains, thus generating stronger hydrogen bonds. A redshift in the absorption maximum (from 1620 to 1615 cm^{-1}) is admit-

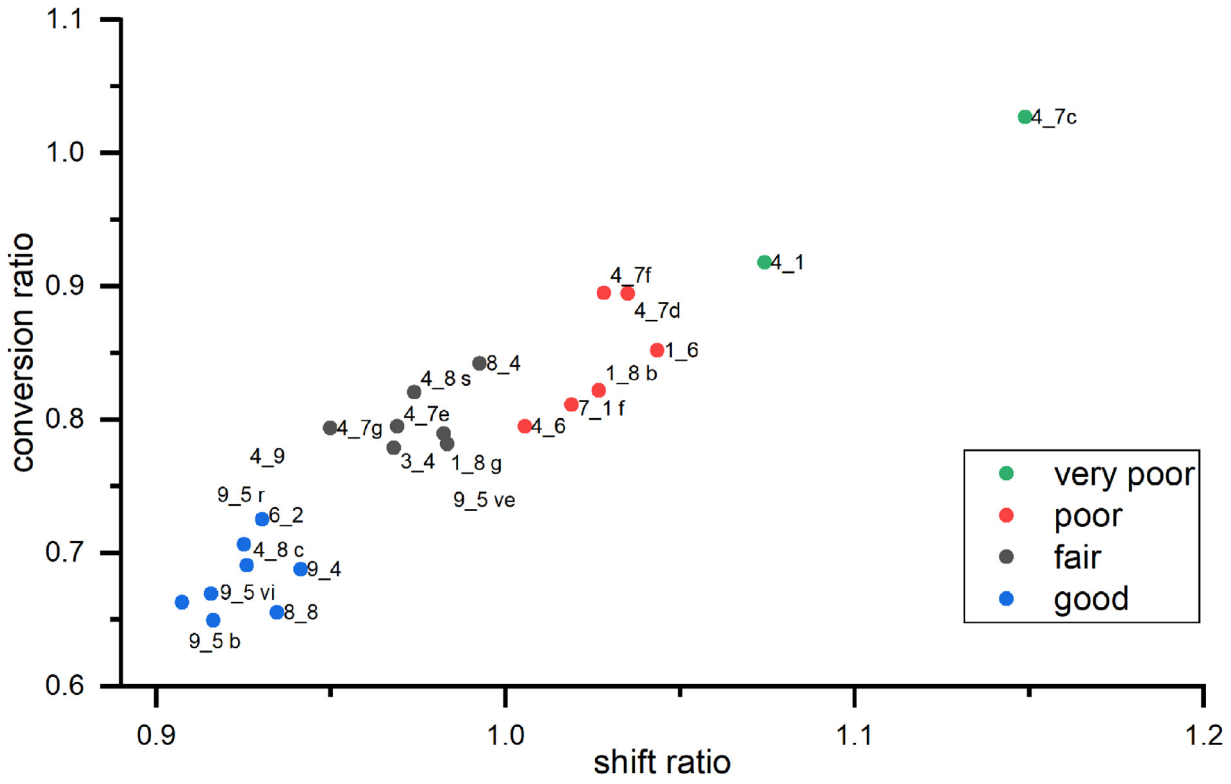

Fig. 3. Shift ratio (R_S) vs conversion ratio (R_C) plot. The samples are coloured according to the estimated condition as reported in the legend.

ted when even stronger H-bond are formed due to the presence of aggregated β-strand [44]. Such structures occur in the amorphous phase surrounding the β-sheet crystallites. However, some authors do not report a division between the contribution of intermolecular β-sheet and β-strand [49]. The relative abundance of crystallites/β-strand thus explains the relationship between the shift of the absorbence maximum and silk deterioration. It is known that, as degradation takes place, UV radiation affects firstly the amorphous phase, whose relative percentage decreases [26,33]. As β-strands disappear, absorption maximum shifts to blue owing to the emergence of β-sheet signals - though with a lower intensity. So, the shift can be related to the degradation in progress. It is important to stress that each spectrum from historical silks can show a different state of degradation and so a different amide shift value for each sample can be expected.

Amide II band also shows different vibrational contributions (Fig. 2). In this case, the conformational information is more difficult to interpretate, as peaks associated to β-sheet and disordered chain are very close (1545 and 1530 cm^{-1}, respectively). On the other hand, tyrosine shows in this region two absorption bands (as reported in Table 2), one at 1555 cm^{-1} which is broad and weak, and the other at 1516 cm^{-1} which is very intense. The amide II peak which appears at around 1510 cm^{-1} originates from the overlapping of the tyrosine peak at 1516 cm^{-1} and of another signal from β-sheets at 1508 cm^{-1}. The amide II peak is also influenced by signals from tyrosine oxidation products [2], mainly dopamine [57,58], which shows a strong peak at 1503 cm^{-1}, with a shoulder at 1466 cm^{-1}. Unlike the shift in amide I caused by the hydrogen bonding strength, the amide II shift is probably due to the fluctuation of the β-sheet signals and to the variation in tyrosine content. The maximum of the amide II corresponds to the absorption of tyrosine for unaged soft silk and sample 6_2. On the contrary, in the spectrum of the sample 4_1 the maximum undergoes a redshift to 1508 cm^{-1} (β-sheet content) and 1503 cm^{-1} (dopamine absorption). At the same time, the contribution of unaffected tyrosine at 1516 cm^{-1} decreases. This trend agrees with literature [59], which reports that the tyrosine content decreases due to dry thermal ageing and especially under UV light exposure (as tyrosine suffers from photo-oxidation [2]). As well as for amide I shift, the conversion of tyrosine cannot directly be linked to the ageing of the silk, as the rate of conversion can be influenced by several factors. Amino acid analysis on historical samples for example showed that light is detrimental for tyrosine [20].

An indicator of the shift (shift ratio – R_S) is obtained by dividing the intensities at 1625 cm^{-1} by the intensities at 1617 cm^{-1}. Similarly, the ratio between 1503 cm^{-1} and 1516 cm^{-1} gives an indicator of the conversion of tyrosine into dopamine (conversion ratio – R_C). By plotting the shift ratio (R_S) vs the conversion ratio (R_C), Fig. 3 is obtained. The two ratios show a linear positive correlation with an R^2 value equal to 0.89. This indicates that the shift of the amide I takes place simultaneously to the conversion of tyrosine. The combination of the two ratios could be defined as degradation index and allows to assess the state of preservation of the samples.

Silk samples appear to be grouped into four groups. As degradation is being evaluated, a label is assigned to each group according to the estimated condition of each sample. The chosen labels are based on the terms which are of common use in condition reports, i.e. good, fair, poor and very poor. These terms refer to the state of preservation of the silk fibre and their assignment is based on visual assessment. It should be stressed that the grouping is tentative because samples show great variability within the group. Each label could be interpreted on the basis of the theory of silk degradation (refer to Theory section).

(i) “Good condition”: this group includes samples which show the amide I maximum at lower wavenumbers. As previously explained, the lowest wavenumber is related to the highest quantity of intermolecular β-sheets or aggregated β-strand,

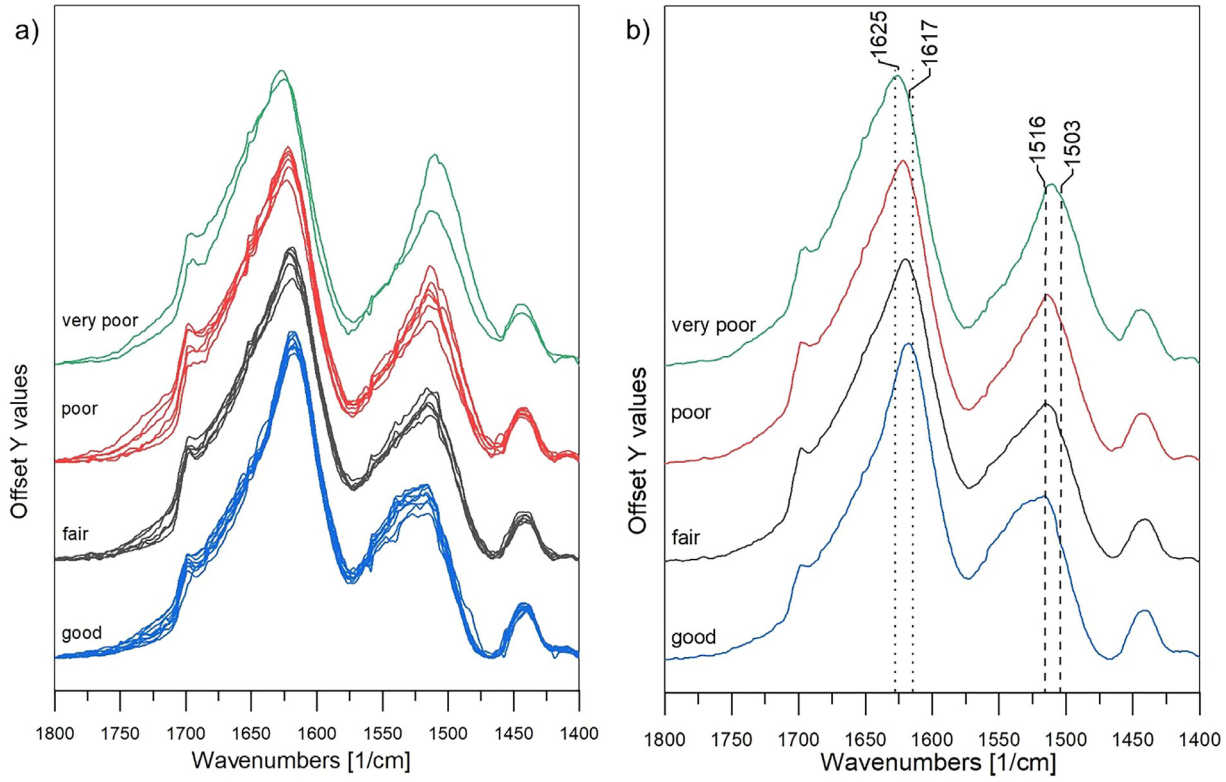

Fig. 4. a) Split of ATR-FTIR spectra of all samples into 4 groups; b) stacked average ATR-FTIR spectra of each group. Every group is labelled according to the estimated condition of its samples.

indicating unaged silk. The spectrum of samples belonging to this group (e.g. sample 6_2) strictly resembles that of the reference unaged degummed silk (Fig. 2). Also, the peak at 1516 cm^{-1} is clearly the maximum in both the sample and the reference, indicating that tyrosine did not suffer from deterioration; hence a low R_C value. According to literature, such silk is in good condition and could be considered as contemporary to our ages. If found on a presumed old textile, it could indicate a recent restoration.

(ii) "Fair condition": this includes silks that underwent slight degradation, limited to aggregated β-strand. The peak maximum shows a slight blueshift due to the disappearance of aggregated β-strand. This silk could be considered as a century-old, so coeval to the artifacts coming from 20th century backwards. This kind of silk is probably contemporary to the armour making, or part of an historical conservation treatment.

(iii) "Poor condition": this group is characterised by a shift ratio above 1 and the signal of amide I at 1622 cm^{-1}. The peak at around 1503 cm^{-1} increases in these samples, due to the conversion of tyrosine into dopamine. A great variability is shown by the samples, probably due to the amount of light to which they were exposed.

(iv) "Very poor condition": in this group, the maximum of amide I is at 1625 cm^{-1} or higher. The intensity of the peak at around 1510 cm^{-1} dramatically increases in these samples, shifting from 1516 cm^{-1}. This is an indicator that tyrosine was converted into its decay product dopamine. This silk appears visibly depolymerized (Figure S1).

The classification into groups which is proposed can be visualized in Fig. 4a,b. On the left, the spectra of the samples are plotted according to the group every sample belongs to. On the right, stacked average spectra of the four groups are shown for clarity. For further reference, overlapped average spectra are plotted in Fig. 6b. It is clear how the evaluation of the grouping is useful as an assessment of the state of preservation of the samples. It should be highlighted that degraded samples are not necessarily the oldest, but they show degradation features that could be caused by intrinsic reasons such as the type of mordants or by the exposure to external factors such as high level of RH, light and heat. Ageing is a time-dependant process which proceeds gradually, so theoretically it could be possible to sort different samples according to a timeline. As the textile collection has recently been musealized, it hardly experienced mild and homogenous environmental conditions. Having been stored in different conditions during their life, each armour has a unique degradation history. For these reasons, it is not possible to establish unequivocal correlations between the sample dating and its state of preservation, although the presumed dating for each sample is generally in good agreement with the deterioration assessment. The results of this process are reported in Table 3. Sometimes, a discrepancy appears between parts which are in very good conditions in comparison to the presumed dating or to other textiles of the armour. This can indicate a possible differentiation between original fibres and fibres added during restoration campaigns.

Fig. 5 shows SEM images of silk references and of a selection of samples from different groups. The integrity of the fibres with different state of preservation were studied by scanning electron microscopy. Major changes occur after degumming (from hard to soft silk). When the sericin-coating of silk fibres is removed by hot soapy water, the smooth and clean fibroin fibres are revealed. Sample 6_2, which is classified as in "good condition", shows a mostly smooth surface, which strictly resembles unaged soft silk.

Table 3
Lists of the samples, indicating the main characteristics of the manufact and the estimated condition status. When there is a discrepancy between the proposed dating and the condition status, the sample name is in italic. NA means that it was not possible to obtain a condition assessment due to the presence of other materials. Samples are expected to have been irradiated by sunlight during their life, unless "internal" is specified.

Sample	Presumed dating (century)	Condition status	Colour	Armour part	Textile typology
1_6	late 16th	poor/very poor	orange	*kabuto*	tassel
1_8b	late 16th	poor	light blue	*nodowa*	brocade lining (two colours)
1_8 g	late 16th	fair	orange	*nodowa*	brocade lining (two colours)
3_4	17th	fair	green	*kote*	brocade lining
4_1	18th	very poor	orange	*kabuto*	chin cord
4_6	18th	poor	blue	*kote*	embroidered lining
4_7c	18th	very poor	yellow	*kote*	embroidery thread on 4_6
4_7d	18th	poor	light blue	*kote*	embroidery thread on 4_6
4_7e	18th	poor	blue	*kote*	embroidery thread on 4_6
4_7f	18th	poor/very poor	white	*kote*	embroidery thread on 4_6
4_7 g	18th	good/fair	blue	*kote*	embroidery thread on 4_6
4_8c	18th	good	bright orange	*kabuto*	tassel (internal)
4_8s	18th	fair	dark orange	*kabuto*	tassel
4_9	18th	good	golden yellow	*haidate*	embroidery thread on light blue brocade
4_10a	late 16th	NA (other material)	blue	*suneate*	internal lining
4_10b	late 16th	NA (other material)	yellow	*suneate*	internal lining
6_2	early 20th	good	yellow	*sode*	tassel
7_1f	late 16th	poor	orange	*kote*	sewing thread
7_1a	late 16th	NA (other material)	light blue	*kote*	brocade lining (two colours)
7_1b	late 16th	NA (other material)	orange	*kote*	brocade lining (two colours)
8_4	17th	fair/poor	green	*suneate*	sewing thread
8_8	17th	good	light orange	*kabuto (shikoro)*	lacing braid
9_2	late 19th	NA (other material)	bright orange	*kabuto (shikoro)*	lacing braid
9_4	late 19th	good	bright orange	*kabuto (shikoro)*	lacing braid
9_5a	late 19th	good	white	*kabuto (shikoro)*	lacing braid
9_5b	late 19th	good	bluish violet	*kabuto (shikoro)*	lacing braid
9_5c	late 19th	fair	green	*kabuto (shikoro)*	lacing braid
9_5d	late 19th	good	pink	*kabuto (shikoro)*	lacing braid

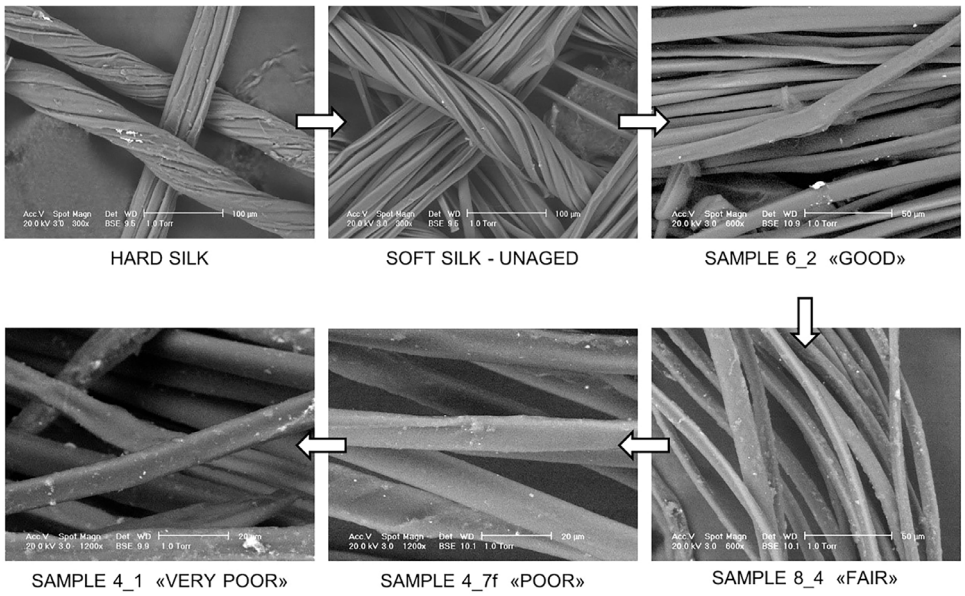

Fig. 5. SEM images (BSE mode) of different kinds of silk (hard/soft silk) and of soft silk at different decay stages. White arrows suggest the decay flow. Every sample from the armour collection is labelled with the estimated condition status.

As more aged real samples are considered, notable differences appear on the surface of the fibroin fibres. The samples chosen from the groups "fair", "poor" and "very poor", showed roughness. These unravelled microfibers detaching from the main fibre can be interpreted as structural damage in the fibre [60]. These irregularities reflect the degradation produced by the ageing [20]. No clear differences amongst early and advanced stages of ageing appear. The results obtained from the SEM observation enable to differentiate between well-preserved silk and others, and agree with the spectroscopic evaluation.

5.3. Classification according to Principal Component Analysis (multivariate method)

The two-variables visualization of data proved to be successful in assessing the deterioration of samples. Also a multivariate approach was tested to evaluate if the same results could be obtained. In particular, Principal Component Analysis (PCA) could offer an easier-to-use approach. A matrix **X** was constructed of the x_i objects (samples) for n variables (wavenumbers) across the whole spectral range. The first PCA model highlighted that some sam-

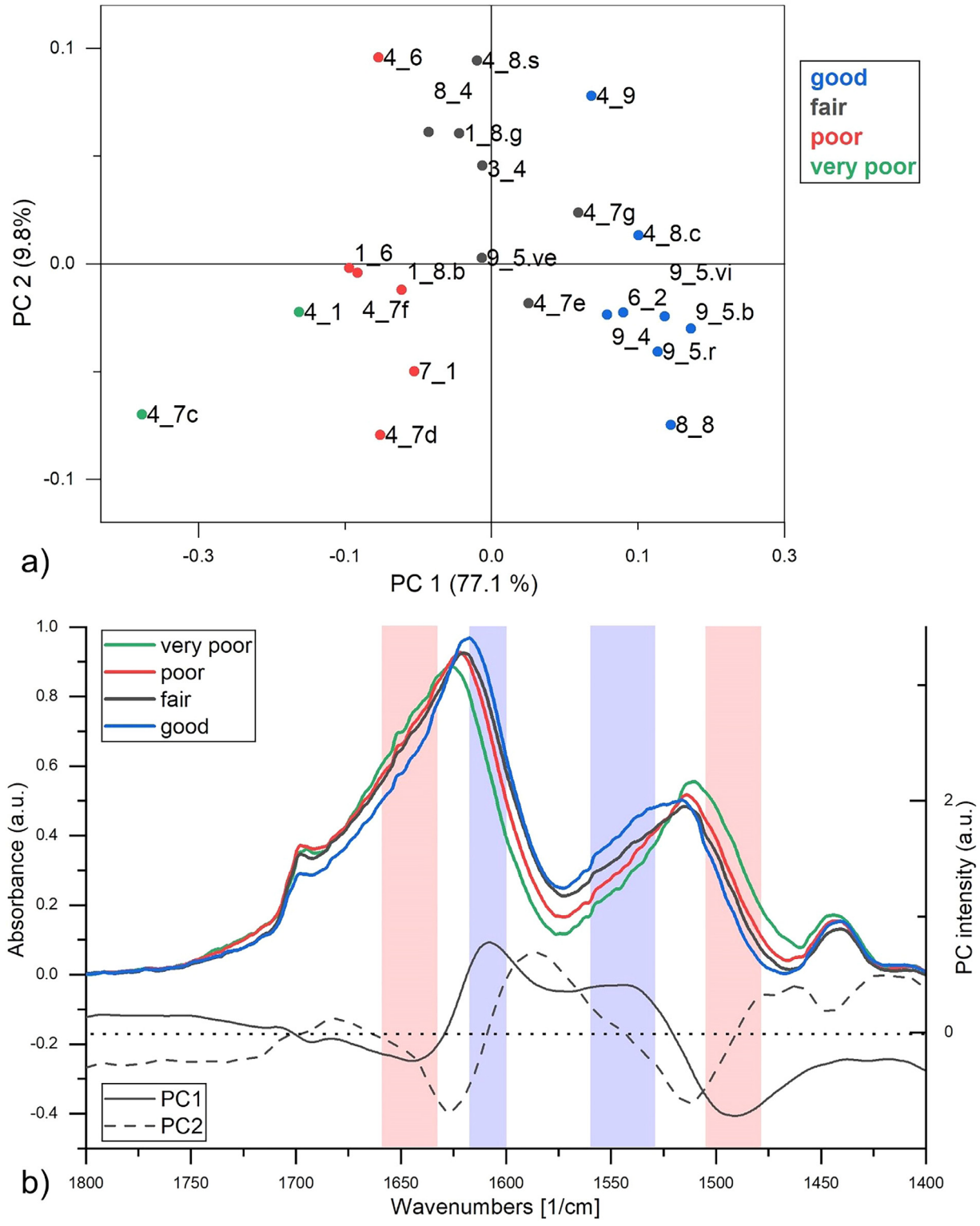

Fig. 6. a) PCA score plot of PC1 and PC2; b) relative loading plot of PC1 and PC2 with the averaged ATR-FTIR spectra of the four groups. The samples and the spectra are coloured according to the estimated condition status as reported in the legend.

ples (4_10b, 4_10g, 7_1b, 7_1g), which manifested signals from extraneous materials, are very different from all the others (Figure S2); these samples strongly influenced both PC1 and PC2, so they were excluded from further chemometric calculation. Their peculiar characteristics are fully presented in Appendix B. To enhance the information contained in amide I and II bands, a matrix with a reduced spectral range (1800 – 1400 cm^{-1}) was constructed, excluding the outliers samples and sample 9_2, as it showed peculiar signals appeared in the region of interest (see Appendix B).

The score plot is presented in Fig. 6a, where the samples labels are coloured according to the groups which were previously introduced. Samples belonging to the “good” group correspond to positive values on PC1 (77.1% of variance), while “very poor” samples to the negative ones. Samples which are assigned to “fair” and

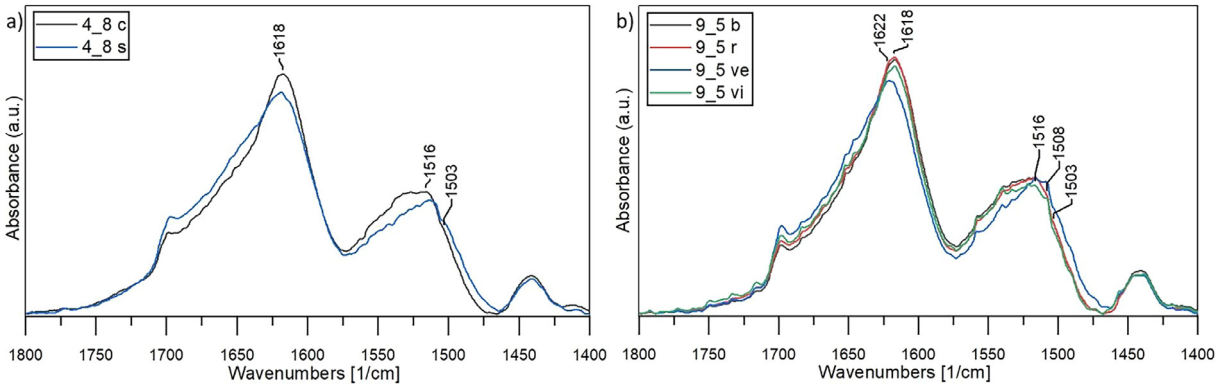

Fig. 7. a) ATR-FTIR spectra of samples 4_8c,s (region between 1800 and 1400 cm^{-1}); b) ATR-FTIR spectra of samples 9_5a,b,c,d (region between 1800 and 1400 cm^{-1}).

"poor" groups are placed according to their state of preservation. Thus, samples are located along PC1 according to the degradation stage, demonstrating that it is possible to correlate spectra to the physical deterioration of silk samples. PCA do not provide a classification but an effective and objective clustering. Studying the loadings plot allows to evaluate the most important spectral regions involved. Loadings values are shown as line plot (wavelength vs loading value for each PC) and compared with the spectra. In Fig. 6b, the loadings of PC1 are shown together with the mean spectra of the four groups. Positive loading values are located at around 1610 and 1560–1540 cm^{-1}, where the bands of "good" samples can be found. These positive values are associated to a higher contribution from tyrosine (1555 cm^{-1}), α-helix/disordered structures (1540 cm^{-1}), and aggregated β-strand/tyrosine (1608 cm^{-1}). All these contributions decrease with ageing [45]. Negative loading values appear at around 1645 and 1490 cm^{-1}. As expected, they are characteristic for the "poor" and "very poor" samples. As previously discussed, these samples share a high contribution from α-helix/random coil structures (1645 cm^{-1}) and the signals coming from tyrosine conversion into dopamine [57], which shows a strong peak at 1503 cm^{-1}, with a shoulder at 1466 cm^{-1}. It clearly appears from the averaged spectra that the contribute from this band at around 1490 cm^{-1} increases with the degradation of silk samples.

Along PC2 (9.8% of explained variance) in the scores plot, a group of samples would seem to deviate towards positive values of the axis (samples 4_6, 4_8 s, 4_9, 8_4, 1_8g, 3_4). Observing the PC2 loadings in Fig. 6b, loading values show a trend which strictly resembles to the spectrum of silk itself. The reason of this behaviour could be probably related to the instrumental variability. It was demonstrated [31] that silk differences in the texture and in the thickness of silk threads can affect the intensity of signal.

In summary, PC1 allows to distinguish samples according to the shifts in amide I peak and in the ratio tyrosine/dopamine. It is significant that PCA assigns to samples the same state of preservation which was found previously by evaluating the degradation index (Fig. 3). PCA is an unsupervised learning method, so it is able to identify similarities in spectra with objectivity. Based on these two types of results, we can suggest a condition evaluation for each analysed sample, whose results are shown in Table 3. As previously stated, the condition of a sample cannot be related directly to an absolute dating. However, it is interesting to compare both the information to detect materials which are probably not contemporary with the armour. This can be seen in samples 4_8c, 4_9, and 8_8. After defining the condition of the samples, it is straightforward to identify the components showing better conservation condition than the rest of the textiles of the armour. In this way, it could be possible to distinguish the components belonging to recent restoration(s) and the ones assignable to the original manufacturing. The original parts have a higher historical value as the life of the armour was marked by periodic renovation due to wear and tear [6]. On the other hand, having detected the strong damage associated to some samples is essential to organise targeted restoration works or, in the specifical case of samurai armours, to know if it would be appropriate to produce supports to carry the weight of metallic parts of the armour without putting the degraded textiles under stress.

5.4. Differences in ageing behaviour

Different light exposure conditions can produce high variations in the condition of the fibres. This is supported by Fig. 7a, which shows the spectra of samples 4_8c and 4_8s, taken from the same part of the armour Mor.004, but from different areas of a tassel. These two regions of the tassel had presumably a different exposure to light, as they are respectively the inner and the outer parts of the tassel. As a matter of fact, their appearance shows that they have faded to a different extent. Sample 4_8s comes from the outer part of the tassel, which experienced colour fading, while 4_8c shows a darker hue and comes from the inner part, which was protected from light as the tassel is quite thick. In early stages of ageing, UV light affects mainly tyrosine, which suffers from photo-oxidation. The subsequent formation of radicals begins the degradation of the polypeptide chain [2]. Consequently, the outer silk suffered more damage and sample 4_8s is characterized by a dull aspect. The slight change at 1620 cm^{-1} indicates the decrease of the signal of aggregated strands and confirms that the sample is in an early deterioration stage. Amide II signal reveals more about degradation: tyrosine contribution at 1516 cm^{-1} decreased in the outer silk (sample 8_4s). Similarly, the growth in the peak at 1503 cm^{-1} confirms the rise in the contribution of dopamine. All this information agrees with the sources of variability on PC1, and the two samples place themselves accordingly in PCA score plot (Fig. 6a).

To complete the analysis of the amides I and II spectral range it is interesting to consider the dyes influence on silk ageing. Fig. 7b shows the spectral region 1800–1400 cm^{-1} from the spectra of the four threads which were braided to form a multicoloured braid (sample 9_5b,r,ve,vi). The position of the samples is the same for all of them, suggesting that the exposure to light is the same. Similarly, it is unlikely that only the threads of a particular colour were replaced in a past conservation treatment. Nevertheless, sample 9_5ve differs from the others, as also indicated by PCA (Fig. 6a). As no other differences amongst these samples exist, we can suppose that the source of variability is due to the dye or mordant. This difference during the manufacturing process could led sample

9_5ve to an accelerated ageing, as suggested by a previous work [21]. This hypothesis will be tested extensively in a future work. Similar conclusions could be suggested for samples 4_7, 4_7c, 4_7d, 4_7e, 4_7f, and 4_7g, which are thread of an embroidery work on a sleeve of armour Mor.004, and for sample 1_8g and 1_8b, which are warp and weft of the same textile.

6. Conclusions

A qualitative condition evaluation of silk samples from an historical collection was suggested, based on ATR-FTIR analysis. The evaluation of the spectra aimed to find trends in recurrent peaks shifts which appeared from the visual comparison of the peaks. By plotting the ratios calculated from the intensities at specific wavenumbers, it was possible to assign for each sample a condition evaluation: good, fair, poor and very poor. In order to develop a multivariate alternative, we demonstrated that Principal Component Analysis (PCA) gives a qualitative deterioration assessment based on the same theoretical basis. PCA appears to be a simple and effective way to evaluate the state of conservation; this method is even more valuable when dealing with a large number of samples. When a few samples are analysed, the visual evaluation of the shift in amide I and II peaks can give a qualitative indication of the state of preservation. The conservator's interest for this kind of information is evident as it could suggest appropriate conservation, display, and storage strategies. The work also shows that external factors such as light exposure, dyes and mordants can deeply influence the degradation rate, implying that the deterioration stage cannot be directly related to the ageing time. As a consequence, the degradation index cannot be related to an absolute dating of the samples. Yet, the condition assessment along with other scientific analyses, e.g. the investigation of dyes, can be used to obtain information about the dating by making comparisons between the state of preservation and the presumed dating of each manufact. Discrepancies suggests that materials which were though as original could have been added during conservation campaigns or that the presumed dating should be revised. The correspondence between the condition and the dating suggests that the latter is accurate.

Acknowledgments

The authors would like to acknowledge 'Centro Tessile Serico Sostenibile' (Como, Italy) for providing the reference samples of silk; Valentina Risdonne and Lucia Burgio (Conservation Department, Victoria and Albert Museum, Cromwell Road, South Kensington, London SW7 8 2RL, UK) for generously giving their time and sharing their knowledge during the revision of the manuscript.

Supplementary materials

Supplementary material associated with this article can be found, in the online version, at doi:10.1016/j.culher.2024.01.015.

Appendix A

The Collection was donated to the Museo delle Culture Lugano (MUSEC) in 2017 by the collector Paolo Morigi, who already owned one Japanese armour (2017.Mor.4) and acquired all the others in two auctions held in Nice and Paris in June 2016. The Collection was presented in a temporary exhibition at the MUSEC in 2018 and is now permanently on display there.

Japanese armours with different style and from different periods can be found within the Collection. All the armours are *kinsei gusoku*, ("modern time armour") which date back to different historical ages: the Azuchi-Momoyama period, the harshest period of feudal wars in Japan spanning for all the second half of the 16th century; the peaceful Edo period (1603–1868); the Meiji period (1868–1912); the Taishō period (1912–1926); the Shōwa period (1926–1989). Some of them (2017.Mor.1 and 2017.Mor.7) are battle armours of the Azuchi-Momoyama period and made to be tested in the battlefields, so they are anatomically shaped, and comfortable to wear. The others were made when armours were used for celebrations and parades only. Some of them still have some war-tested elements made in the previous period, for example the helmet (*kabuto*) of 2017.Mor.3 and 2017.Mor.8, as well as his greaves (*suneate*). Armour 2017.Mor.4 and 2017.Mor.9 are *kinsei gusoku* made according to the old-fashioned style (*mukashi gusoku*, "once upon a time armour") used in the Middle Ages.

Armour silk textiles showed a great variability in colours and type. Samples were categorised from the armour part which comes from, as follows: tassel, brocade lining, chin cord, embroidered lining, embroidered thread, internal lining, sewing thread, lacing braid. A schematised image reporting the main parts of the traditional samurai armours is shown in Fig. A1.

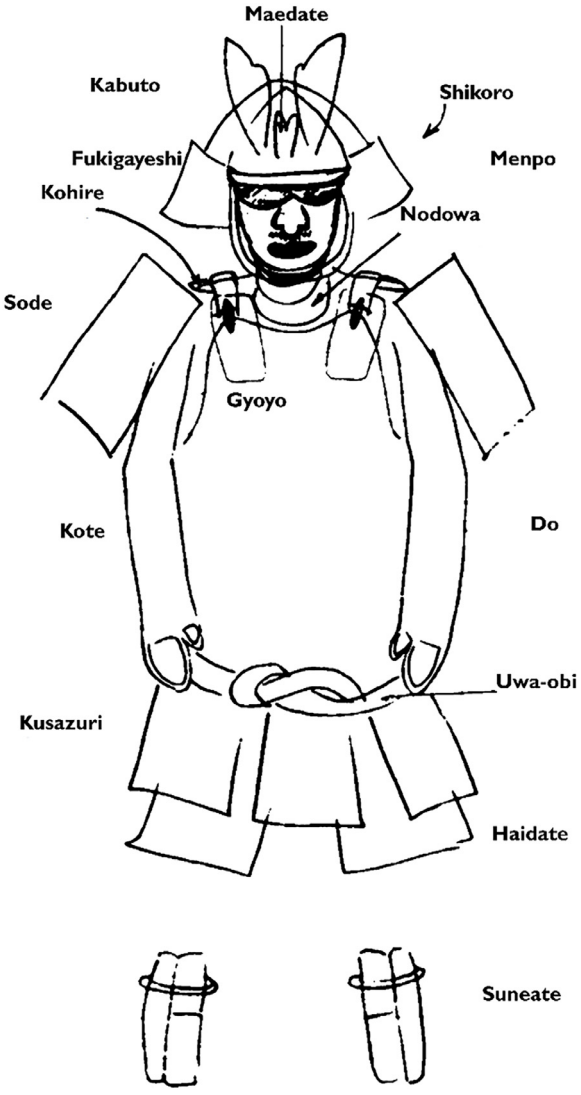

Fig. A1. The main parts of the traditional samurai armour.

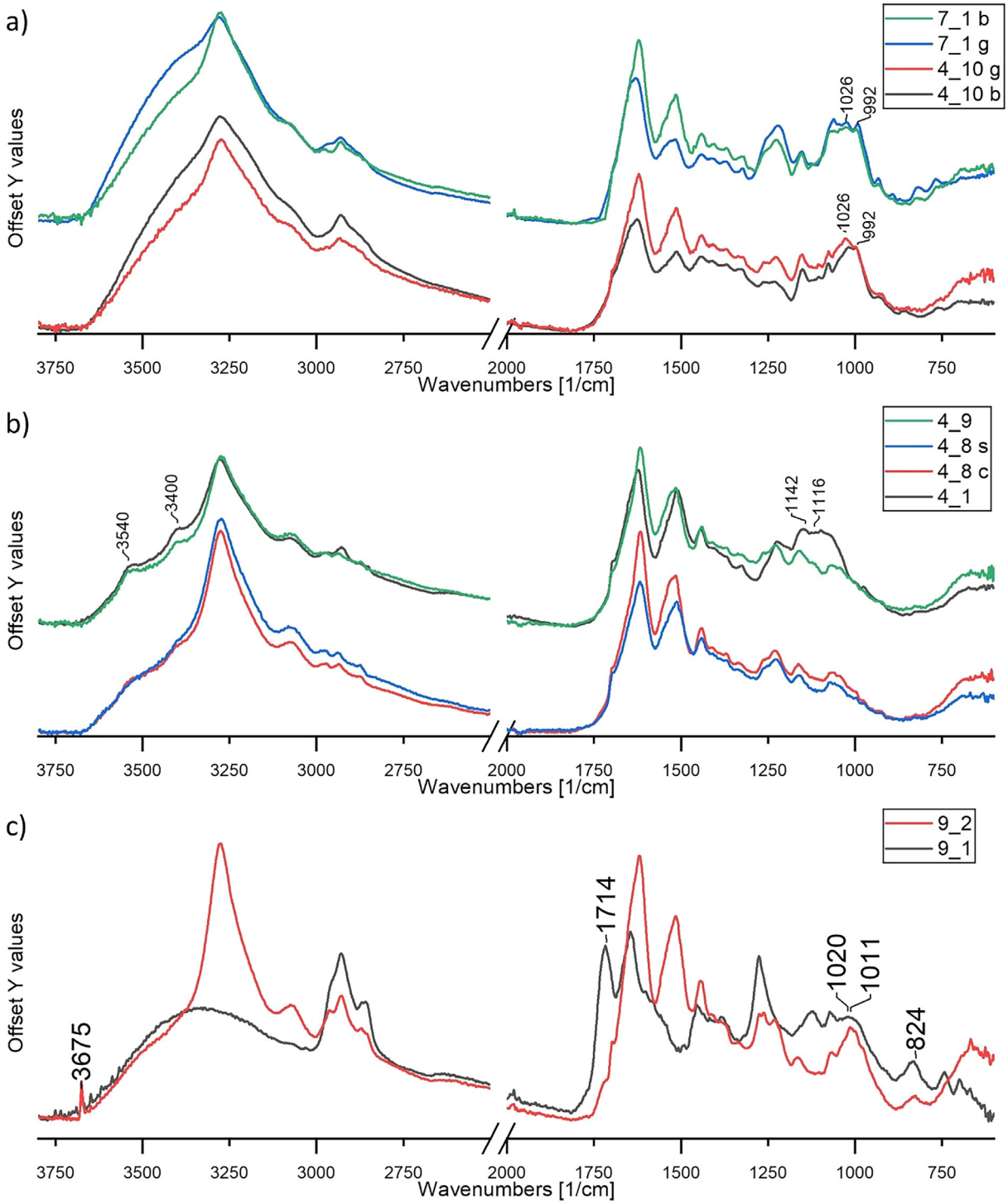

Fig. B1. ATR-IR spectra of peculiar samples: spectra with similar features are grouped together.

Appendix B

The presence of other materials was evaluated in the peculiar samples, whose spectra are shown in Fig. B1. Similar spectra are grouped together.

Samples 4_10b (blue-dyed), 4_10g (yellow-dyed), 7_1b (blue-dyed) and 7_1g (orange-dyed) show a broad absorption band around 1000 cm^{-1} which probably comes from polysaccharide-rich substances, as starch [61] (Fig. B1a); it is not clear whether the polysaccharide-rich substance is derived from dirt or due to a manufacturing process, such as sugar weighting [2,62]. Samples 4_1, 4_8c/s, and 4_9 show the spectral features of gypsum (3530, 3400, 1142, 1116 cm^{-1}) [63] (Fig. B1b). The presence of calcium and sulfur is confirmed by EDX analysis and is consistent with the use of $CaSO_4$ as a weighting agent, but it can be related also to a transformation process of a calcium salt (e.g. $CaCO_3$) under the action of gaseous pollutants (SO_2), or to some mineral dust adhering to the surface [64,65]. The possibility that signals could be related to deterioration products was also investigated, as it was suggested in previous literature [66]. However, no products which

are considered to be related to silk deterioration [2] have been recognized. In Fig. B1c, the spectrum of sample 9_2 is shown together with the spectrum of gilt metal plates surrounding the textile (sample 9_1). In both the rosin signals appear (1714, 824 and 1011 cm^{-1})[61] and talc (3676 and 1020 cm^{-1}) [63], whose presence is hardly comprehensible. Nevertheless, thanks to the study of other materials of the armours, it is possible to hypothesise an interpretation. The samples were taken from the lacing (*odoshi-ge*) amongst metal plates, which in armour Mor.9 are golden. Analyses on gilt metal plates revealed that they are covered with a layer of rosin, and additionally showing the characteristic signal of talc. As such materials are generally considered extraneous to Japanese handicraft tradition, we can expect that their presence is due to a past conservation treatment, which probably was focused on the gilding. Rosin contaminated the textile which lays very close to the metal plates, and talc was a contaminant for the rosin, as they are very frequently mixed and sold together as a powder which is used, for example, in printmaking as a sizing agent [67].

References

[1] P. Garside, Understanding and improving the durability of textiles, in: P.A. Annis (Ed.), Durability of Historic Textiles, Woodhead Publishing Limited, Cambridge, UK, 2012, pp. 184–204.

[2] A. Timar-Balazsy, D. Eastop, Materials, in: Chemical Principles in Textile Conservation, Third, Routledge, New York, NY, USA, 1998, pp. 3–66.

[3] V.A., Textiles and clothing along the silk roads, United Nations educational, scientific and cultural organization (UNESCO) and China National Silk Museum (CNSM), Paris (France) and Hangzhou, Zhejiang (China), 2022.

[4] S. Desrosiers, in: Scrutinizing Raw Material Between China and Italy: the Various Processing Sequences of Bombyx Mori Silk, L'Atelier Du Centre de Recherches Historiques [En Ligne], 2019, p. 20, doi:10.4000/acrh.10323.

[5] F. Civita, Le sete e le lacche vanno in battaglia: le armature giapponesi, in: M. Luraschi (Ed.), Il Samurai. Da Guerriero a Icona, Silvana Editoriale, Cinisello Balsamo, Italy, 2018, pp. 80–87.

[6] C.M. Breeze, Preventative Conservation of Samurai Armor, Andover, Massachusetts, USA, 2008.

[7] E.-A. Haldane, L. Hillyer, D. Kalsi, The conservation and display of Indian textiles at the victoria and albert museum, in: S. Jose, S. Thomas, P. Pandit, R. Pandey (Eds.), Handbook of Museum Textiles, Volume 1: Conservation and Cultural Research, John Wiley and Sons, Hoboken, New Jersey, USA, 2022, pp. 291–314.

[8] P. Garside, The role of fibre identification in textile conservation, in: M.M. Houck (Ed.), Identification of Textile Fibers, Cambridge -, Woodhead Publishing, Boca Raton, Florida, USA, 2009, pp. 335–365, doi:10.1533/9781845695651.3.335.

[9] L. Geminiani, F.P. Campione, C. Corti, M. Luraschi, S. Mo-, S. Recchia, L. Rampazzi, Differentiating natural and modified cellulosic fibres by ATR- FTIR spectroscopy, Heritage 5 (2022) 4114–4139, doi:10.3390/heritage5040213.

[10] P. Peets, I. Leito, J. Pelt, S. Vahur, Identification and classification of textile fibres using ATR-FT-IR spectroscopy with chemometric methods, Spectrochim. Acta a Mol. Biomol. Spectrosc. 173 (2017) 175–181, doi:10.1016/j.saa.2016.09.007.

[11] M. Asai, M. Tsuboi, T. Shimanouchi, Infrared spectra of polypeptides and related compounds, J. Phys. Chem. 59 (1964) 322–325.

[12] T. Miyazawa, E.R. Blout, The infrared spectra of polypeptides in various conformations: amide I and II bands, J. Am. Chem. Soc. 83 (1961) 712–719, doi:10.1021/ja01464a042.

[13] A. Barth, Infrared spectroscopy of proteins, Biochim. Biophys. Acta Bioenerg. 1767 (2007) 1073–1101, doi:10.1016/j.bbabio.2007.06.004.

[14] J. de Meutter, E. Goormaghtigh, Amino acid side chain contribution to protein FTIR spectra: impact on secondary structure evaluation, Eur. Biophys. J. 50 (2021) 641–651, doi:10.1007/s00249-021-01507-7.

[15] B. Hernández, F. Pflüger, A. Adenier, S.G. Kruglik, M. Ghomi, Vibrational analysis of amino acids and short peptides in hydrated media. VIII. Amino acids with aromatic side chains: l-phenylalanine, l-tyrosine, and l-tryptophan, J. Phys. Chem. B 114 (2010) 15319–15330, doi:10.1021/jp106786j.

[16] P.H.Setyarini Purnomo, D. Sulistyaningsih, Degradation behavior of silk fibroin biomaterials - a review, J. Eng. Sci. Technol. Review 12 (2019) 67–74, doi:10.25103/jestr.125.08.

[17] P. Garside, S. Lahlil, P. Wyeth, Characterization of historic silk by Polarized attenuated total reflectance fourier transform infrared spectroscopy for informed conservation, Appl Spectrosc. 59 (2005) 1242–1247.

[18] R.L. Feller, Accelerated Ageing - Photochemical and Thermal Aspects, The Getty Conservation Institute, Ann Arbor, Michigan, USA, 1994.

[19] E. Bramanti, E. Benedetti, Determination of the secondary structure of isomeric forms of human serum albumin by a particular frequency deconvolution procedure applied to fourier transform IR analysis, Biopolymers 38 (1996) 639–653, doi:10.1002/(SICI)1097-0282(199605)38:5⟨639::AID-BIP8⟩3.0.CO;2-T.

[20] M.Y. Li, Y. Zhao, T. Tong, X.H. Hou, B.S. Fang, S.Q. Wu, X.Y. Shen, H. Tong, Study of the degradation mechanism of Chinese historic silk (Bombyx mori) for the purpose of conservation, Polym. Degrad. Stab. 98 (2013) 727–735, doi:10.1016/j.polymdegradstab.2012.12.021.

[21] D. Badillo-Sanchez, D. Chelazzi, R. Giorgi, A. Cincinelli, P. Baglioni, Understanding the structural degradation of South American historical silk: a Focal Plane Array (FPA) FTIR and multivariate analysis, Sci. Rep. 9 (2019), doi:10.1038/s41598-019-53763-5.

[22] M.A. Koperska, D. Pawcenis, J. Bagniuk, M.M. Zaitz, M. Missori, T. Łojewski, J. Łojewska, Degradation markers of fibroin in silk through infrared spectroscopy, Polym. Degrad. Stab. 105 (2014) 185–196, doi:10.1016/j.polymdegradstab.2014.04.008.

[23] J. Shao, J. Zheng, J. Liu, C.M. Carr, Fourier transform Raman and Fourier transform infrared spectroscopy studies of silk fibroin, J. Appl. Polym. Sci. 96 (2005) 1999–2004, doi:10.1002/app.21346.

[24] X. Luo, J. Wu, A. Intisar, J. Geng, L. Wu, K. Zheng, Y. Du, Study on light aging of silk fabric by fourier transform infrared spectroscopy and principal component analysis, Anal. Lett. 45 (2012) 1286–1296, doi:10.1080/00032719.2012.673098.

[25] A. Serrano, A. Brokerhof, B. Ankersmit, M. van Bommel, From the bottom of the sea to the display case: a study into the long-term preservation of archaeological maritime silk textiles in controlled atmosphere, J. Cult. Herit. 45 (2020) 91–100, doi:10.1016/j.culher.2020.04.004.

[26] P. Garside, P. Wyeth, Crystallinity and degradation of silk: correlations between analytical signatures and physical condition on ageing, Appl. Phys. a Mater. Sci. Process. 89 (2007) 871–876, doi:10.1007/s00339-007-4218-z.

[27] F. Vilaplana, J. Nilsson, D.V.P. Sommer, S. Karlsson, Analytical markers for silk degradation: comparing historic silk and silk artificially aged in different environments, Anal. Bioanal. Chem. 407 (2015) 1433–1449, doi:10.1007/s00216-014-8361-z.

[28] L. Geminiani, F.P. Campione, C. Corti, S. Motella, L. Rampazzi, S. Recchia, M. Luraschi, Unveiling the complexity of Japanese metallic threads, Heritage 4 (2021) 4017–4039, doi:10.3390/heritage4040221.

[29] L. Geminiani, F.P. Campione, C. Canevali, C. Corti, B. Giussani, G. Gorla, M. Luraschi, S. Recchia, L. Rampazzi, Historical silk: a novel method to evaluate degumming with non-invasive infrared spectroscopy and spectral deconvolution, Materials. (Basel) (2023) 16, doi:10.3390/ma16051819.

[30] F. Menges, Spectragryph - optical spectroscopy software, Version 1.2.15, (2021).

[31] M. Boulet-Audet, T. Buffeteau, S. Boudreault, N. Daugey, M. Pézolet, Quantitative determination of band distortions in diamond attenuated total reflectance infrared spectra, J. Phys. Chem. B 114 (2010) 8255–8261, doi:10.1021/jp101763y.

[32] X. Liu, K.-Q. Zhang, Silk fiber — molecular formation mechanism, structure-property relationship and advanced applications, in: C. Lesieur (Ed.), Oligomerization of Chemical and Biological Compounds, IntechOpen, London, UK, 2014, pp. 69–102.

[33] R. Chen, M. Hu, H. Zheng, H. Yang, L. Zhou, Y. Zhou, Z. Peng, Z. Hu, B. Wang, Proteomics and immunology provide insight into the degradation mechanism of historic and artificially aged silk, Anal. Chem. 92 (2020) 2435–2442, doi:10.1021/acs.analchem.9b03616.

[34] H. Liu, S. Zhao, Q. Zhang, T. Yeerken, W. Yu, Secondary structure transformation and mechanical properties of silk fibers by ultraviolet irradiation and water, Textile Res. J. 89 (2019) 2802–2812, doi:10.1177/0040517518803788.

[35] J. Magoshi, Y. Magoshi, S. Nakamura, N. Kasai, M. Kakudo, Physical properties and structure of silk. Thermal behavior of silk fibroin in the random-coil conformation, J Polym. Sci. Polym. Phys. Ed. 15 (1977) 1675–1683, doi:10.1002/pol.1977.180150915.

[36] L. Jeong, K.Y. Lee, J.W. Liu, W.H. Park, Time-resolved structural investigation of regenerated silk fibroin nanofibers treated with solvent vapor, Int. J. Biol. Macromol. 38 (2006) 140–144, doi:10.1016/j.ijbiomac.2006.02.009.

[37] N. v Bhat, S.M. Ahirrao, Investigation of the Structure of Silk Film Regenerated with Lithium Thiocyanate Solution, Polym. Chem. 21 (5) (1983) 1273–1280, doi:10.1002/pol.1983.170210504.

[38] X. Chen, Z. Shao, N.S. Marinkovic, L.M. Miller, P. Zhou, M.R. Chance, Conformation transition kinetics of regenerated Bombyx mori silk fibroin membrane monitored by time-resolved FTIR spectroscopy, Biophys. Chem. 89 (2001) 25–34, doi:10.1016/S0301-4622(00)00213-1.

[39] M. Tsukada, G. Freddi, P. Monti, A. Bertoluzza, N. Kasai, Structure and molecular conformation of tussah silk fibroin films: effect of methanol, J. Polymer Sci. 33 (1995) 1995–2001, doi:10.1002/polb.1995.090331402.

[40] J. Magoshi, M. Mizuide, Y. Magoshi, Physical properties and structure of silk. VI. Conformational changes in silk fibroin induced by immersion in water at 2 to 130°C, J. Polymer Sci. 17 (1979) 515–520.

[41] X. Chen, D.P. Knight, Z. Shao, β-turn formation during the conformation transition in silk fibroin, Soft Matter 5 (2009) 2777–2781, doi:10.1039/b900908f.

[42] W. Lamoolphak, W. De-Eknamkul, A. Shotipruk, Hydrothermal production and characterization of protein and amino acids from silk waste, Bioresour. Technol. 99 (2008) 7678–7685, doi:10.1016/j.biortech.2008.01.072.

[43] D. Pawcenis, M. Smoleń, M.A. Aksamit-Koperska, T. Łojewski, J. Łojewska, Evaluating the impact of different exogenous factors on silk textiles deterioration with use of size exclusion chromatography, Appl. Phys. a Mater. Sci. Process. 122 (2016), doi:10.1007/s00339-016-0052-5.

[44] X. Hu, D. Kaplan, P. Cebe, Determining beta-sheet crystallinity in fibrous proteins by thermal analysis and infrared spectroscopy, Macromolecules.Macromolecules. 39 (2006) 6161–6170, doi:10.1021/ma0610109.

[45] D. Badillo-Sanchez, D. Chelazzi, R. Giorgi, A. Cincinelli, P. Baglioni, Characterization of the secondary structure of degummed Bombyx mori silk in modern

and historical samples, Polym. Degrad. Stab. 157 (2018) 53–62, doi:10.1016/j.polymdegradstab.2018.09.022.
[46] J. Kong, S. Yu, Fourier transform infrared spectroscopic analysis of protein secondary structures, Acta Biochim. Biophys. Sin. (Shanghai) 39 (2007) 549–559, doi:10.1111/j.1745-7270.2007.00320.x.
[47] S. Ling, Z. Qi, D.P. Knight, Z. Shao, X. Chen, Synchrotron FTIR microspectroscopy of single natural silk fibers, Biomacromolecules 12 (2011) 3344–3349, doi:10.1021/bm2006032.
[48] H. Yoshimizu, T. Asakura, The Structure of Bombyx mori Silk Fibroin Membrane Swollen by Water Studied with ESR, 13C-NMR, and FT-IR Spectroscopies, J. Appl. Polym. Sci. 40 (1990) 1745–1756, doi:10.1090/gsm/146/03.
[49] M. Jackson, H.H. Mantsch, Protein secondary structure from FT-IR spectroscopy: correlation with dihedral angles from three-dimensional Ramachandran plots, Can. J. Chem. 69 (1991) 1639–1642, doi:10.1139/v91-240.
[50] P. Taddei, P. Monti, Vibrational infrared conformational studies of model peptides representing the semicrystalline domains of Bombyx mori silk fibroin, Biopolymers 78 (2005) 249–258, doi:10.1002/bip.20275.
[51] M. Boulet-Audet, T. Lefèvre, T. Buffeteau, M. Pézolet, Attenuated total reflection infrared spectroscopy: an efficient technique to quantitatively determine the orientation and conformation of proteins in single silk fibers, Appl. Spectrosc. 62 (2008) 956–962, doi:10.1366/000370208785793380.
[52] E. Goormaghtigh, J.M. Ruysschaert, V. Raussens, Evaluation of the information content in infrared spectra for protein secondary structure determination, Biophys. J. 90 (2006) 2946–2957, doi:10.1529/biophysj.105.072017.
[53] M. Sonoyama, T. Nakano, Infrared rheo - optics of bombyx mori fibroin film by dynamic step - scan FT - IR spectroscopy combined with Digital SIgnal Processing, Appl. Spectrosc. 54 (2000) 968–973.
[54] E. Van Nimmen, K. De Clerck, J. Verschuren, K. Gellynck, T. Gheysens, J. Mertens, L. Van Langenhove, FT-IR spectroscopy of spider and silkworm silks. Part I. Different sampling techniques, Vib. Spectrosc. 46 (2008) 63–68, doi:10.1016/j.vibspec.2007.10.003.
[55] S. Akyuz, T. Akyuz, B. Cakan, S. Basaran, Investigations of the historic textiles excavated from Ancient Ainos (Enez - Turkey) by multiple analytical techniques Dedicated to Professor Simion Simon, J. Mol. Struct. 1073 (2014) 37–43, doi:10.1016/j.molstruc.2014.03.068.
[56] J. Grdadolnik, ATR-FTIR spectroscopy: its advantages and limitations, Acta Chim.Slov 49 (2002) 631–642.
[57] C. Giulivi, N.J. Traaseth, K.J.A. Davies, Tyrosine oxidation products: analysis and biological relevance, Amino Acids 25 (2003) 227–232, doi:10.1007/s00726-003-0013-0.
[58] C. Solazzo, J.M. Dyer, S. Deb-Choudhury, S. Clerens, P. Wyeth, Proteomic profiling of the photo-oxidation of silk fibroin: implications for historic tin-weighted silk, Photochem. Photobiol. (2012) 1217–1226, doi:10.1111/j.1751-1097.2012.01167.x.
[59] X. Zhang, I. vanden Berghe, P. Wyeth, Heat and moisture promoted deterioration of raw silk estimated by amino acid analysis, J. Cult. Herit. 12 (2011) 408–411, doi:10.1016/j.culher.2011.03.002.
[60] G. Carissimi, A.A. Lozano-Pérez, M.G. Montalbán, S.D. Aznar-Cervantes, J.L. Cenis, G. Víllora, Revealing the influence of the degumming process in the properties of silk fibroin nanoparticles, Polymers. (Basel) (2019) 11, doi:10.3390/polym11122045.
[61] M. Derrick, D. Stulik, J. Laundry, Infrared Spectroscopy in Conservation Science, The Getty Conservation Institute, Los Angeles, USA, 1999.
[62] M. Hacke, Weighted silk: history, analysis and conservation, Stud. Conserv. 53 (2008) 3–15, doi:10.1179/sic.2008.53.supplement-2.3.
[63] N.v. Chukanov, Infrared Spectra of Mineral Species - Extended library, Springer, 2014, doi:10.1007/978-94-007-7128-4_2.
[64] P. Uring, A. Chabas, S.C. Alfaro, Textile ageing due to atmospheric gases and particles in indoor cultural heritage, Environ. Sci. Pollut. Res. 28 (2021) 66340–66354, doi:10.1007/s11356-021-15274-7.
[65] P. Uring, A. Chabas, S. Alfaro, Dust deposition on textile and its evolution in indoor cultural heritage, Eur. Phys. J. Plus. 134 (2019), doi:10.1140/epjp/i2019-12671-5.
[66] M.A. Koperska, T. Łojewski, J. Łojewska, Evaluating degradation of silk's fibroin by attenuated total reflectance infrared spectroscopy: case study of ancient banners from Polish collections, Spectrochim. Acta a Mol. Biomol. Spectrosc. 135 (2015) 576–582, doi:10.1016/j.saa.2014.05.030.
[67] J. Ross, C. Romano, T. Ross, The Complete Printmaker: Techniques, Traditions, Innovations, The Free Press, New York, NY, USA, 1990.